ACCOUNTS of chemical research

Article

pubs.acs.org/accounts

Surface Functionalization of Metal Nanoparticles by Conjugated Metal−Ligand Interfacial Bonds: Impacts on Intraparticle Charge Transfer

Peiguang Hu,[†] Limei Chen,[†] Xiongwu Kang,[‡] and Shaowei Chen*[,†]

[†]Department of Chemistry and Biochemistry, University of California, 1156 High Street, Santa Cruz, California 95064, United States

[‡]New Energy Research Institute, School of Environment and Energy, South China University of Technology, Guangzhou Higher Education Mega Center, Guangzhou, Guangdong 510006, China

CONSPECTUS: Noble metal nanoparticles represent a unique class of functional nanomaterials with physical and chemical properties that deviate markedly from those of their atomic and bulk forms. In order to stabilize the nanoparticles and further manipulate the materials properties, surface functionalization with organic molecules has been utilized as a powerful tool. Among those, mercapto derivatives have been used extensively as the ligands of choice for nanoparticle surface functionalization by taking advantage of the strong affinity of thiol moieties to transition metal surfaces forming (polar) metal−thiolate linkages. Yet, the nanoparticle material properties are generally discussed within the context of the two structural components, the metal cores and the organic capping layers, whereas the impacts of the metal−sulfur interfacial bonds are largely ignored because of the lack of interesting chemistry. In recent years, it has been found that metal nanoparticles may also be functionalized by stable metal−carbon (or even -nitrogen) covalent bonds. Because of the formation of dπ−pπ interactions between the transition-metal nanoparticles and terminal carbon moieties, the interfacial resistance at the metal−ligand interface is markedly reduced, leading to the emergence of unprecedented optical and electronic properties.

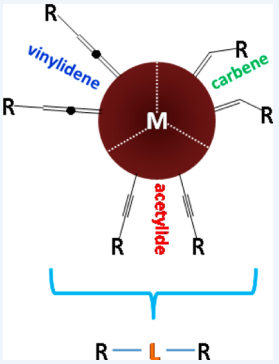

In this Account, we summarize recent progress in the studies of metal nanoparticles functionalized by conjugated metal−ligand interfacial bonds that include metal−carbene (M═C) and metal−acetylide (M−C≡)/metal−vinylidene (M═C═C) bonds. Such interfacial bonds are readily formed by ligand self-assembly onto nanoparticle metal cores. The resulting nanoparticles exhibit apparent intraparticle charge delocalization between the particle-bound functional moieties, leading to the emergence of optical and electronic properties that are analogous to those of their dimeric counterparts, as manifested in spectroscopic and electrochemical measurements. This is first highlighted by ferrocene-functionalized nanoparticles that exhibit nanoparticle-mediated intervalence charge transfer (IVCT) among the particle-bound ferrocenyl moieties, as manifested in electrochemical and spectroscopic measurements. Such intraparticle charge delocalization has also been observed with other functional moieties such as pyrene and anthracene, where the photoluminescence emissions are consistent with those of their dimeric derivatives. Importantly, as such electronic communication occurs via a through-bond pathway, it may be readily manipulated by the valence states of the nanoparticle cores as well as specific binding of selective molecules/ions to the organic capping shells. These fundamental insights may be exploited for diverse applications, ranging from chemical sensing to (nano)electronics and fuel cell electrochemistry. Several examples are included, such as sensitive detection of nitroaromatic derivatives, metal cations, and fluoride anions by fluorophore-functionalized metal nanoparticles, fabrication of nanoparticle-bridged molecular dyads by, for instance, using nanoparticles cofunctionalized with 4-ethynyl-*N*,*N*-diphenyl-aniline (electron donor) and 9-vinylanthracene (electron acceptor), and enhanced electrocatalytic activity of acetylene derivatives-functionalized metal/alloy nanoparticles for oxygen reduction reaction by manipulation of the metal core electron density and hence interactions with reaction intermediates. We conclude this Account with a perspective where inspiration from conventional organometallic chemistry may be exploited for more complicated nanoparticle surface functionalization through the formation of diverse metal−nonmetal bonds. This is a unique platform for ready manipulation of nanoparticle properties and applications.

INTRODUCTION

Recently a wide variety of metal−ligand bonds have been formed and used to functionalize metal nanoparticles,[1−9] beyond the conventional metal−thiolate (M−S) linkages.[10] This is primarily motivated by results from earlier studies of the adsorption of hydrocarbons on transition-metal surfaces.[11,12] The bonding interactions are generally believed to involve dπ−pπ interactions between the transition metals and the terminal carbon moieties.[13−15] For instance, metal−carbon (M−C═) covalent bonds can be readily formed by using aryl diazonium as the precursors which exhibit significantly reduced interfacial resistance, as compared to the M−S counterparts.[16−18] Metal−carbene (M═C) π bonds are formed by using diazo derivatives as the capping ligands,[19,20] and metal−acetylide (M−C≡)/−vinylidene (M═C═C−) bonds are produced by the self-

Received: July 20, 2016
Published: October 3, 2016

DOI: 10.1021/acs.accounts.6b00377
Acc. Chem. Res. 2016, 49, 2251−2260

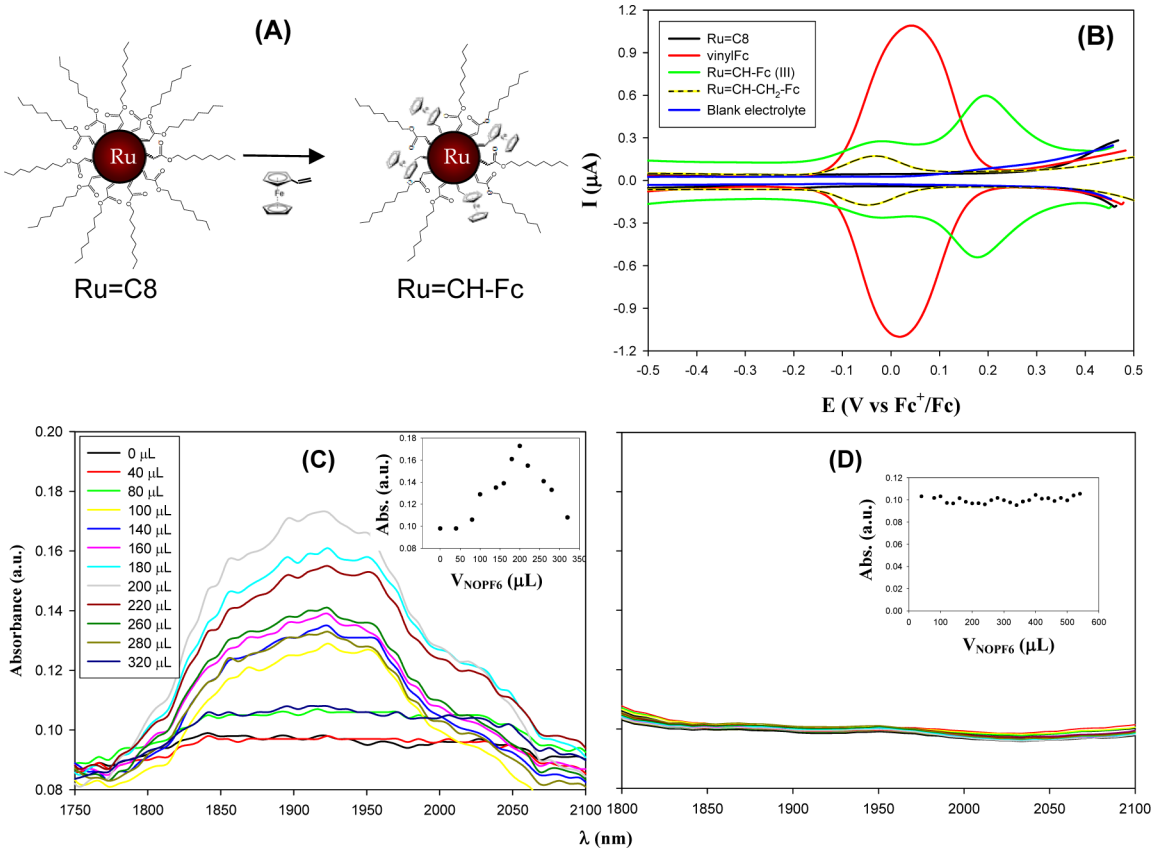

Figure 1. (A) Preparation of Ru=CH−Fc from Ru=C8 nanoparticles by olefin metathesis reaction with vinylferrocene. (B) SWVs of vinylferrocene monomers (red), Ru=C8, Ru=CH−Fc (sample III), and Ru=CH−CH_2−Fc nanoparticles in 0.1 M TBAP in DMF. NIR spectra of (C) Ru=CH−Fc (sample III) and (D) Ru=CH−CH_2−Fc nanoparticles with the addition of varied amounts of 1 mM $NOPF_6$ (specificed in figure legends). Insets show the variation of the absorbance at 1930 nm with the amount of $NOPF_6$ added (variations of particle concentrations are corrected). Adapted with permission from ref 19. Copyright 2008 American Chemical Society.

assembly of acetylene derivatives onto transition-metal surfaces.[4,5,18,21−24] More recently, it has been found that olefin derivatives may also be exploited as new capping ligands for nanoparticle surface functionalization, as a result of platinum-catalyzed dehydrogenation, such that the produced acetylene moieties self-assemble onto the nanoparticle surfaces.[25,26] Of these, the formation of conjugated metal−carbon interfacial bonds is found to endow the nanoparticles with unprecedented optical, electronic and electrochemical properties, due to effective intraparticle charge delocalization among the nanoparticle-bound functional moieties.[4,17,19,25,27−29] Importantly, this may be readily manipulated by the electronic properties of the metal cores which serve as part of the chemical bridge for intraparticle charge transfer.[30,31] In addition, when multiple functional moieties are incorporated onto the same nanoparticle surface, specific electronic interactions with selective molecules/ions may also be exploited as an effective variable in gating the intraparticle charge transfer,[32−34] a platform that has the potential for chemical sensing of specific molecules/ions[35,36] and deliberate manipulation of the nanoparticle electrocatalytic activity in fuel cell electrochemistry.[1,22−24,37−39]

In this Account, we will highlight these recent breakthroughs in the surface functionalization of metal nanoparticles with conjugated metal−ligand interfacial bonds and the impacts on intraparticle charge transfer. Interparticle charge transfer has also been found to vary with the metal−ligand interfacial bonding interactions, which has been summarized in an earlier review,[40] and will not be repeated here.

INTRAPARTICLE CHARGE DELOCALIZATION

One unique property arising from conjugated metal−ligand interfacial bonds is nanoparticle-mediated intraparticle charge delocalization. This is first demonstrated with carbene-capped nanoparticles, where diazo derivatives self-assemble onto "bare" metal colloids synthesized by thermolytic reduction of metal salts in 1,2-propanediol forming M=C π bonds,[19,41−45] and the resulting nanoparticles may undergo olefin metathesis reactions with vinyl derivatives for further surface functionalization.[3,17,19,27,35] Experimentally, multiple ferrocene moieties are incorporated onto a ruthenium nanoparticle surface by olefin metathesis reactions of carbene-functionalized ruthenium (Ru=C8) nanoparticles with vinylferrocene (Figure 1A).[19] Square wave voltammetric (SWV) measurements[19] of the resulting Ru=CH−Fc nanoparticles (Figure 1B) show two pairs of voltammetric peaks with the formal potentials ($E^{\circ\prime}$) at −0.019 and +0.185 V (vs Fc^+/Fc), corresponding to a potential spacing ($\Delta E^{\circ\prime}$) of 0.204 V (which remains rather consistent with the ferrocene surface coverage varied from 5% to 20%, as determined by NMR measurements). This is consistent with ferrocene oligomers bridged by conjugated linkages,[46,47] and suggests that indeed intervalence charge transfer (IVCT) occurs between the nanoparticle-bound ferrocene moieties thanks to the conjugated Ru=C interfacial bonds. In contrast, when allylferrocene is used instead for the olefin metathesis reaction, only one pair of voltammetric peaks are observed with the resulting Ru=CH−CH_2−Fc nanoparticles, indicating that

DOI: 10.1021/acs.accounts.6b00377
Acc. Chem. Res. 2016, 49, 2251−2260

IVCT is effectively switched off by the saturated Csp^3 spacer, as IVCT occurs by a through-bond mechanism.[48−51] Further confirmation is obtained in near-infrared (NIR) spectroscopic measurements. From Figure 1C and D, it can be seen that with the addition of $NOPF_6$ into the Ru═CH−Fc nanoparticle solution, an absorption peak emerges at around 1930 nm, and the peak intensity shows a volcano-shaped variation with the amount of $NOPF_6$ added. Such a spectroscopic signature has also been observed with ferrocene oligomers at mixed valence.[46,47] In sharp contrast, no apparent NIR response is observed for the Ru═CH−CH_2−Fc nanoparticles, indicating the lack of electronic communication because of the Csp^3 spacers. Similar observations are also obtained with ruthenium nanoparticles passivated by ferrocenyl moieties through Ru−C≡ interfacial bonds.[4]

Intraparticle charge delocalization has also been demonstrated in the manipulation of nanoparticle optical properties. For instance, when fluorophores such as pyrene[27] and anthracene[17] are bonded onto ruthenium nanoparticle surfaces by Ru═C π bonds, the nanoparticles exhibit photoluminescence emissions that are consistent with those of the dimeric counterparts, suggesting extended conjugation between the particle-bound fluorophores. In contrast, with the incorporation of a saturated carbon spacer, the photoluminescence resembles those of the fluorophore monomers.

New optical properties have also been observed when metal nanoparticles are functionalized with acetylide fragments forming M−C≡ π bonds.[4] Ruthenium nanoparticles capped with 1-octynide (Ru−OC) are used as the illustrating example (Figure 2A inset), which are prepared by superhydride reduction of $RuCl_3$ in the presence of 1-octynyllithium.[4] In FTIR measurements, the C≡C stretch is found to red-shift to 1936 cm^{-1} from 2119 cm^{-1} observed for 1-octyne monomers (Figure 2A), which is ascribed to the decreased bonding order as a result of intraparticle charge delocalization through the conducting metal cores. In fact, the Ru−OC nanoparticles exhibit apparent photoluminescence emission (Figure 2B) that is analogous to that of diacetylene derivatives (−C≡C−C≡C−).[52]

Similar photoluminescence is observed with (intact) *n*-alkynes-capped metal nanoparticles.[5,18,21,22] This is first demonstrated with ruthenium nanoparticles stabilized by the self-assembly of 1-dodecyne onto "bare" Ru colloid surface,[5,18] which involves the formation of Ru-vinylidene (Ru═C═CH−R) interfacial linkages. This is thought to involve a tautomeric rearrangement process, as confirmed by the specific reactivity of the nanoparticles with imine derivatives forming a heterocyclic complex at the metal−ligand interface.[5] Notably, the resulting nanoparticles can also undergo olefin metathesis reactions with vinyl/acetylene-terminated molecules. In sharp contrast, no such reactivity is observed with 1-dodecynide-stabilized ruthenium nanoparticles, because of the formation of Ru−C≡ dπ bonds instead at the metal−ligand interface. The chemistry has also been extended to other metal nanoparticles including Pt, Pd, AgAu, AuPd, and so forth,[5,18,21−24] where the effects of metal−carbon interfacial bonds on nanoparticle electronic and spectroscopic properties have been studied, both theoretically and experimentally.[8,9,53−59]

For platinum nanoparticles, such metal−ligand interfacial bonds may also be formed by using olefin derivatives as the capping ligands,[25] as a result of platinum-catalyzed dehydrogenation,[25,26] and the resulting nanoparticles exhibit optical and electronic properties analogous to the acetylene-capped

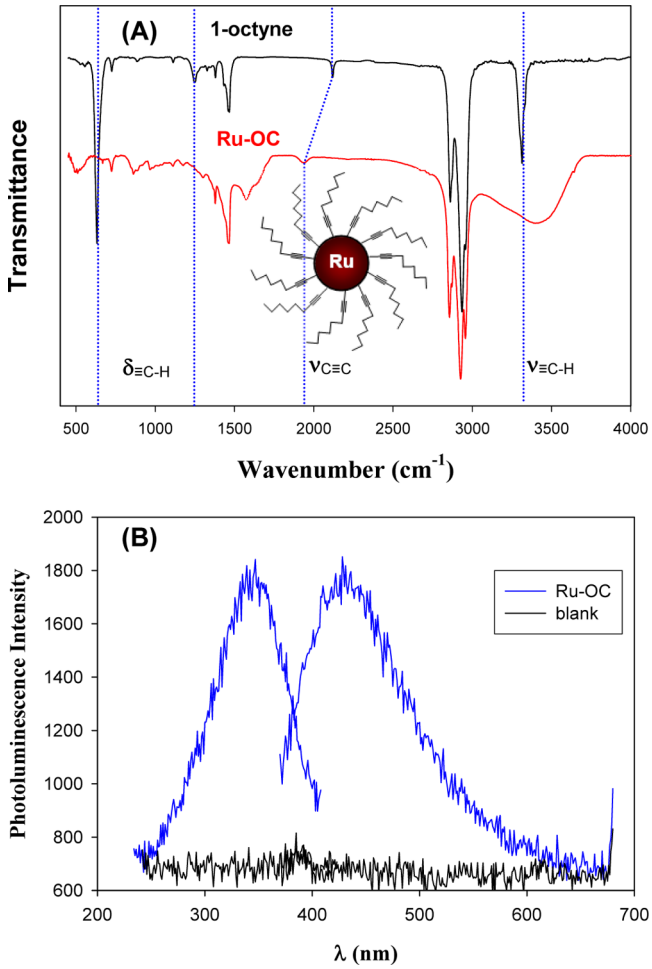

Figure 2. (A) FTIR spectra of 1-octyne and Ru-OC nanoparticles. Inset is a schematic of the Ru-OC nanoparticles. (B) Excitation and emission spectra of Ru-OC nanoparticles in CH_2Cl_2, along with those of the blank solvent. Adapted with permission from ref 4. Copyright 2010 American Chemical Society.

counterparts.[5,18,21,22] X-ray absorption studies show that the interfacial bonding structure is in the intermediate between those of Pt−C_{sp} and Pt−C_{sp2}. In a further study with *para*-substituted styrene derivatives,[26] the chemical reactivity of the ligands is found to vary with the electron-withdrawing properties of the *para*-substituents.

Interfacial reactivity of other ligands has also been exploited for effective intraparticle charge delocalization.[28,29] This has been demonstrated by nanoparticle-catalyzed decarboxylation at the metal−ligand interface, leading to direct bonding of functional moieties onto the nanoparticle surface.

MANIPULATION OF INTRAPARTICLE CHARGE TRANSFER

In the above examples, the nanoparticle cores serve as part of the chemical bridge to facilitate intraparticle charge transfer. Thus, the electronic properties of the nanoparticle cores may serve as a critical variable in manipulating the nanoparticle-mediated electronic communication. Using Ru−OC nanoparticles as an example, we have examined the impacts of the charge states of nanoparticle cores on intraparticle charge delocalization.[30] As the nanoparticles behave as a molecular capacitor,[60] the charge states can be readily achieved by

DOI: 10.1021/acs.accounts.6b00377
Acc. Chem. Res. 2016, 49, 2251−2260

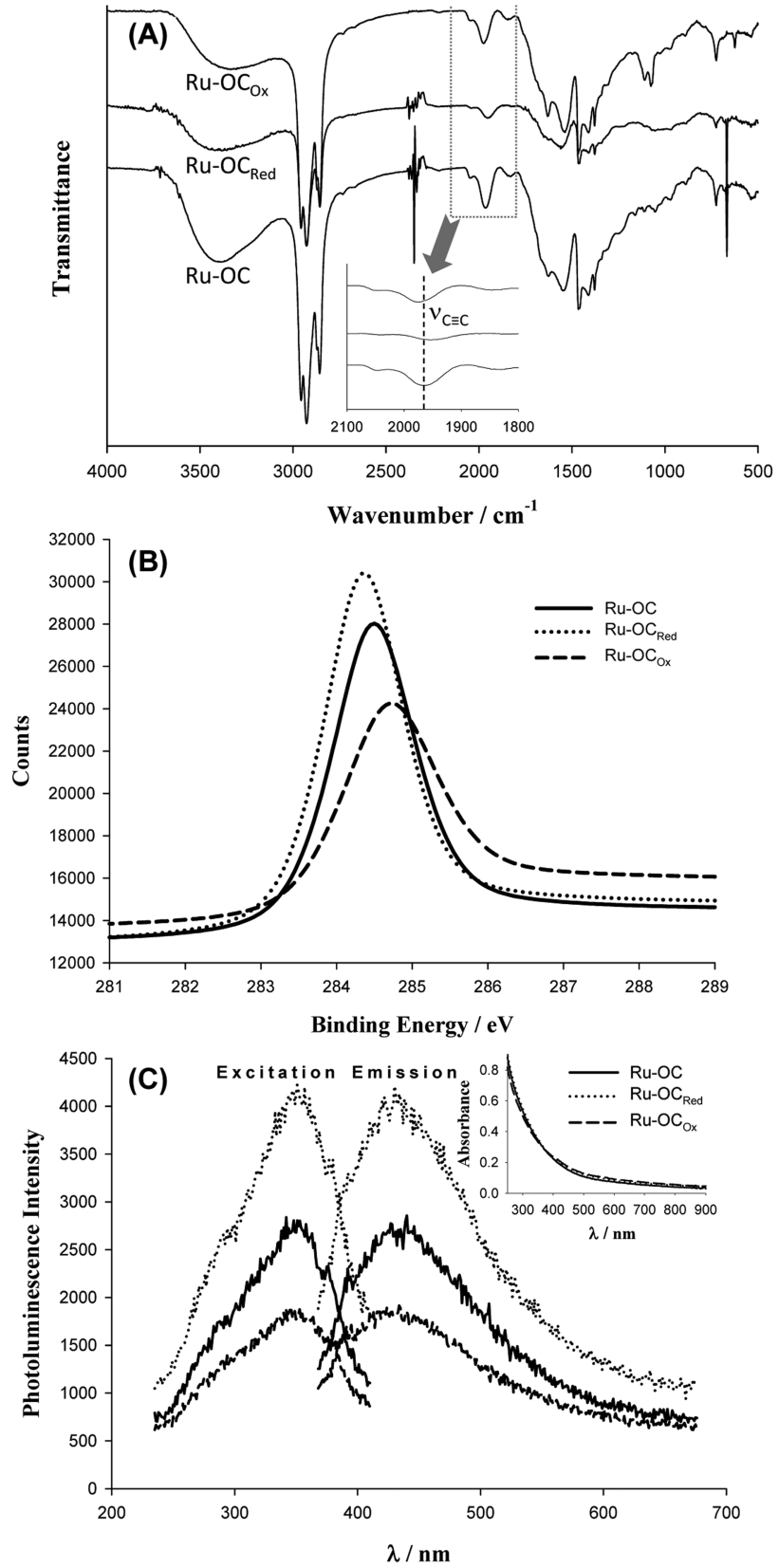

Figure 3. (A) FTIR spectra, (B) XPS spectra of *sp*-hybridized C1*s* electrons, and (C) photoluminescence spectra of Ru-OC, Ru-OC$_{Red}$, and Ru-OC$_{Ox}$ nanoparticles. Inset to (A) magnifies the portions enclosed by the dotted box with the C≡C vibrational stretch highlighted by the dashed line. Inset to (C) shows the corresponding UV−vis absorption spectra of the three nanoparticles in CH_2Cl_2. Adapted with permission from ref 30. Copyright 2010 WILEY-VCH.

DOI: 10.1021/acs.accounts.6b00377
Acc. Chem. Res. 2016, 49, 2251−2260

chemical reduction ($NaBH_4$)/oxidation ($Ce(SO_4)_2$).[30] For the reduced sample ($Ru-OC_{Red}$) electrochemical measurements show that on average each nanoparticle gains 0.67 electron, whereas for the oxidized ones ($Ru-OC_{Ox}$), a loss of 0.63 electron per nanoparticle. Despite the small changes of the nanoparticle charge states, drastic changes are observed of the nanoparticle properties. For instance, FTIR measurements (Figure 3A) show that the C≡C stretch appears at 1965 cm^{-1} for the Ru−OC sample, which red-shifts to 1953 cm^{-1} for $Ru-OC_{Red}$, but blue-shifts to 1977 cm^{-1} for $Ru-OC_{Ox}$. This means that charging of extra electrons into the metal cores further enhances the charge delocalization, leading to a decreased bonding order and red-shift of the C≡C bond, while opposite for chemical oxidation. Consistent results are obtained in XPS measurements (Figure 3B), where the binding energy of the sp-hybridized C 1s electrons is found to increase in the order of $Ru-OC_{Red}$ < Ru−OC < $Ru-OC_{Ox}$, and in photoluminescence measurements (Figure 3C) where the emission intensity increases in the opposite order, $Ru-OC_{Red}$ > Ru−OC > $Ru-OC_{Ox}$. These observations suggest enhanced intraparticle charge delocalization by increasing core electronic density.

Nanoparticle core size has also been found to play an important role.[31] It is well-known that nanoparticles in the subnanometer regime become molecule-like with a nonzero HOMO−LOMO band gap.[60] This will markedly reduce the electrical conductivity of the nanoparticle cores and hence impede nanoparticle-mediated electronic communication; yet under photoirradiation with photon energy greater than the nanoparticle bandgap, intraparticle charge delocalization will occur. This is indeed observed by comparing the spectroscopic and electrochemical properties of two ethynylferrocene-functionalized platinum (PteFc) nanoparticles, which are prepared by ligand exchange reactions of the corresponding triphenylphosphine-capped Pt nanoparticles with ethynylferrocene.[31] One consists of a Pt_{10} core whereas the other Pt_{314}, as determined by MALDI mass spectroscopy and TEM measurements. UV−vis measurements show that the nanoparticle band gaps are 1.0 and 0.4 eV, respectively. FTIR measurements show that the ferrocenyl ring =C−H and Pt=C=C− stretches appear at 3113 and 2109 cm^{-1} for the ethynylferrocene monomers, which red-shift to 3095 and 2060 cm^{-1} for Pt_{10}eFc, and even further to 3092 and 2024 cm^{-1} for Pt_{314}eFc. This is attributed to charge delocalization between the particle-bound ferrocene moieties owing to the conjugated Pt=C=C− interfacial bonds. The fact that a less pronounced red-shift is observed with the smaller Pt_{10}eFc indicates diminished electronic communication between the ferrocenyl groups due to the reduced electronic conductivity of the semiconductor-like metal cores, whereas the larger ones behave analogously to bulk metal.[60] Consistent results are obtained in electrochemical studies. For the Pt_{314}eFc nanoparticles (Figure 4A), two pairs of voltammetric peaks appear in the dark at $E^{\circ\prime}$ = +0.042 and +0.32 V (vs Fc^+/Fc) with $\Delta E^{\circ\prime}$ = 280 mV, consistent with Class II compounds.[48−51] Under UV irradiation, $\Delta E^{\circ\prime}$ remains identical at 280 mV. This is because the larger nanoparticles act like the bulk metal and the electrical conductivity is independent of UV photoirradiation. In contrast, for the Pt_{10}eFc nanoparticles (Figure 4B), although two pairs of voltammetric peaks are also seen in the dark within the same potential range, the peaks can only be distinguished by deconvolution, at $E^{\circ\prime}$ = +0.042 and +0.22 V with a much smaller $\Delta E^{\circ\prime}$ of 0.18 V. This signifies reduced intraparticle charge transfer between the ferrocenyl moieties on the

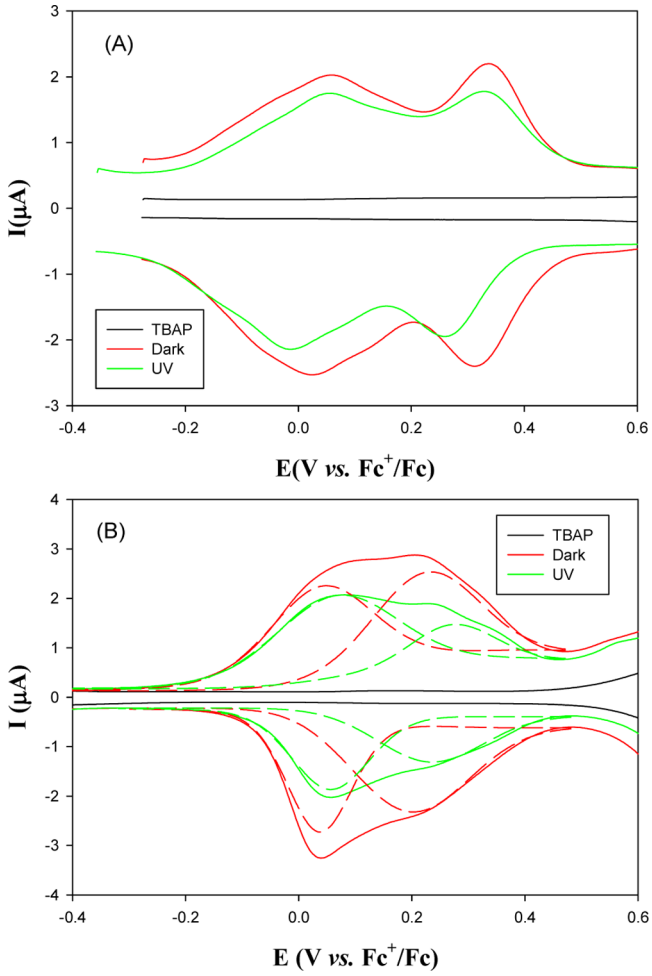

Figure 4. SWVs of (A) Pt_{314}eFc and (B) Pt_{10}eFc nanoparticles at a gold electrode in 0.1 M tetrabutylammonium perchlorate in CH_2Cl_2 in the dark and under UV irradiation. In panel (B), solid curves are experimental data and dashed curves are deconvolution fits. Adapted with permission from ref 31. Copyright 2016 WILEY-VCH.

nanoparticle surface. More interestingly, under UV irradiation the two pairs of voltammetric peaks now appear at +0.060 and +0.26 V with $\Delta E^{\circ\prime}$ increased to 0.20 V, as compared with that (0.18 V) in the dark, suggesting improved electronic conductivity of the semiconductor-like metal cores that results in enhanced intraparticle charge transfer between the particle-bound ferrocenyl moieties. Similar photochemical manipulation of nanoparticle-mediated IVCT is observed with semiconducting nanoparticles such as Si and TiO_2.[61,62]

Manipulation of intraparticle charge delocalization may also be achieved by incorporating multiple functional moieties onto the nanoparticle surface where selective binding to specific molecules/ions can be exploited to impact the electronic density of the nanoparticle cores. For instance, when ruthenium nanoparticles are cofunctionalized with pyrene and histidine derivatives through Ru=C π bonds (synthesized by olefin metathesis reactions of Ru=C8 nanoparticles with their vinyl derivatives, where the surface coverages are estimated by NMR measurements to be 5.3% and 10.5% for the pyrene and histidine moieties, respectively),[33] complexation of the histidine moieties with selective metal ions (e.g., Hg^{2+}, Co^{2+}, and Pb^{2+}) polarizes the nanoparticle core electrons via the π molecular backbone, leading to diminished intraparticle charge delocaliza-

DOI: 10.1021/acs.accounts.6b00377
Acc. Chem. Res. 2016, 49, 2251−2260

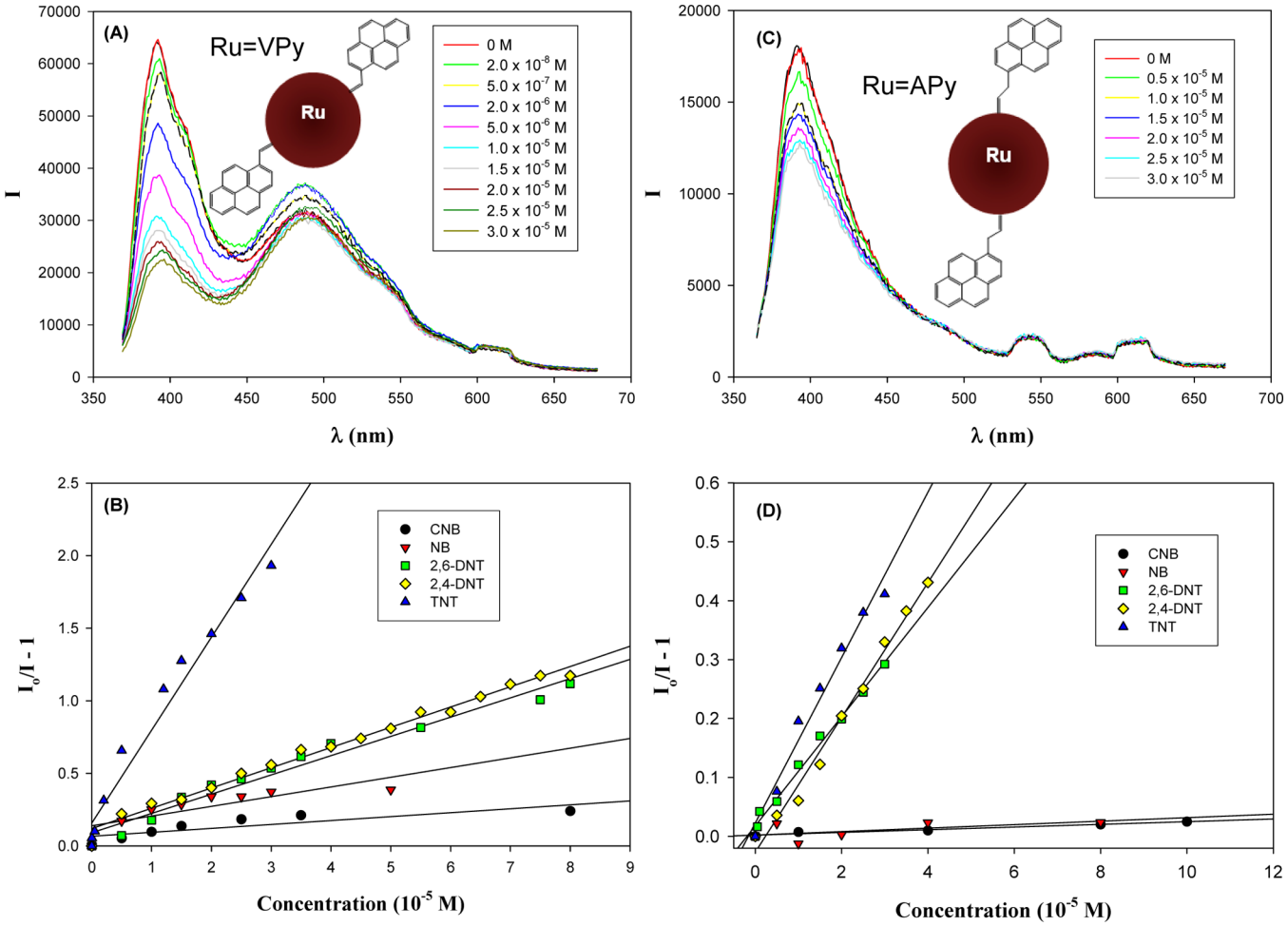

Figure 5. Emission spectra of (A) Ru═VPy and (C) Ru═APy nanoparticles with the addition of varied amounts of TNT. Stern–Volmer plots of the (B) Ru═VPy and (D) Ru═APy nanoparticles in the presence of different nitroaromatic analytes. Insets to (A) and (B) are the schematic illustrations of Ru═VPy and Ru═APy nanoparticles. Adapted with permission from ref 35. Copyright 2010 American Chemical Society.

tion between the particle-bound pyrene moieties and hence a clear variation of the photoluminescence emissions, while no apparent change is observed with other ions such as Li^+, K^+, Rb^+, Mg^{2+}, Ca^{2+}, and Zn^{2+}. Similar behaviors have also been observed with ruthenium nanoparticles cofunctionalized with vinylpyrene and vinylbenzo(crown-ether), where the photoluminescence intensity is apparently reduced when the crown-ether moieties bind to selective alkaline metal ions.[32] Similarly, for Pt nanoparticles fully capped with 4-ethynylphenylboronic acid pinacol ester,[36] the nanoparticles exhibit a clear, selective variation of the photoluminescence emission with F^-, thanks to the specific binding affinity of B_{sp2} to F^-, whereas virtually no change is observed with other (halide) anions.

IMPACTS ON APPLICATIONS

As demonstrated above, with the formation of conjugated metal–ligand interfacial linkages, chemical events that occur at a specific site on the nanoparticle surface may be propagated and even amplified to the entire nanoparticles, resulting in a clear variation of the nanoparticle spectroscopic and electrochemical properties. This may be exploited as a unique platform for diverse applications. For instance, the photoluminescence characteristics of vinylpyrene-functionalized ruthenium (Ru═VPy, 26.4% surface coverage) nanoparticles have been exploited as a sensing mechanism for nitroaromatic derivatives.[35] Among the series of 2,4,6-trinitrotoluene (TNT), 2,4-dinitrotoluene (2,4-DNT), 2,6-dinitrotoluene (2,6-DNT), nitrobenzene (NB), and 1-chloro-nitrobenzene (CNB)), TNT causes the most drastic diminishment of the nanoparticle emission at 390 nm (Figure 5A and B). More importantly, the quenching constants obtained are also much larger than those reported previously with luminescence chemosensors based on quantum dots or conjugated polymers. Furthermore, although similar behaviors are also observed with the allylpyrene-functionalized counterparts (Ru═APy, 22.9% surface coverage), the decay is not as significant as for Ru═VPy (Figure 5C and D), which is ascribed to intraparticle charge delocalization in Ru═VPy that improves the electron/energy transfer from the pyrene moieties to the quencher molecules, similar to the amplification effects observed with pyrene-based conjugated polymers. This may enrich the platforms for metal nanoparticle-based chemosensors.[63−68]

Conjugated metal–ligand interfacial bonds may also be exploited for the fabrication of nanoparticle-mediated molecular dyads.[69,70] Experimentally, decyne-capped Ru nanoparticles undergo ligand-exchange reactions with 4-ethynyl-*N*,*N*-diphenylaniline (EDPA), vinylanthracene (VAN), or both to produce Ru(EDPA), Ru(VAN), and Ru(EDPA/VAN) nanoparticles (Figure 6, right panels[34]). Effective intraparticle charge transfer is found to occur from EDPA to VAN in Ru(EDPA/VAN)

DOI: 10.1021/acs.accounts.6b00377
Acc. Chem. Res. 2016, 49, 2251−2260

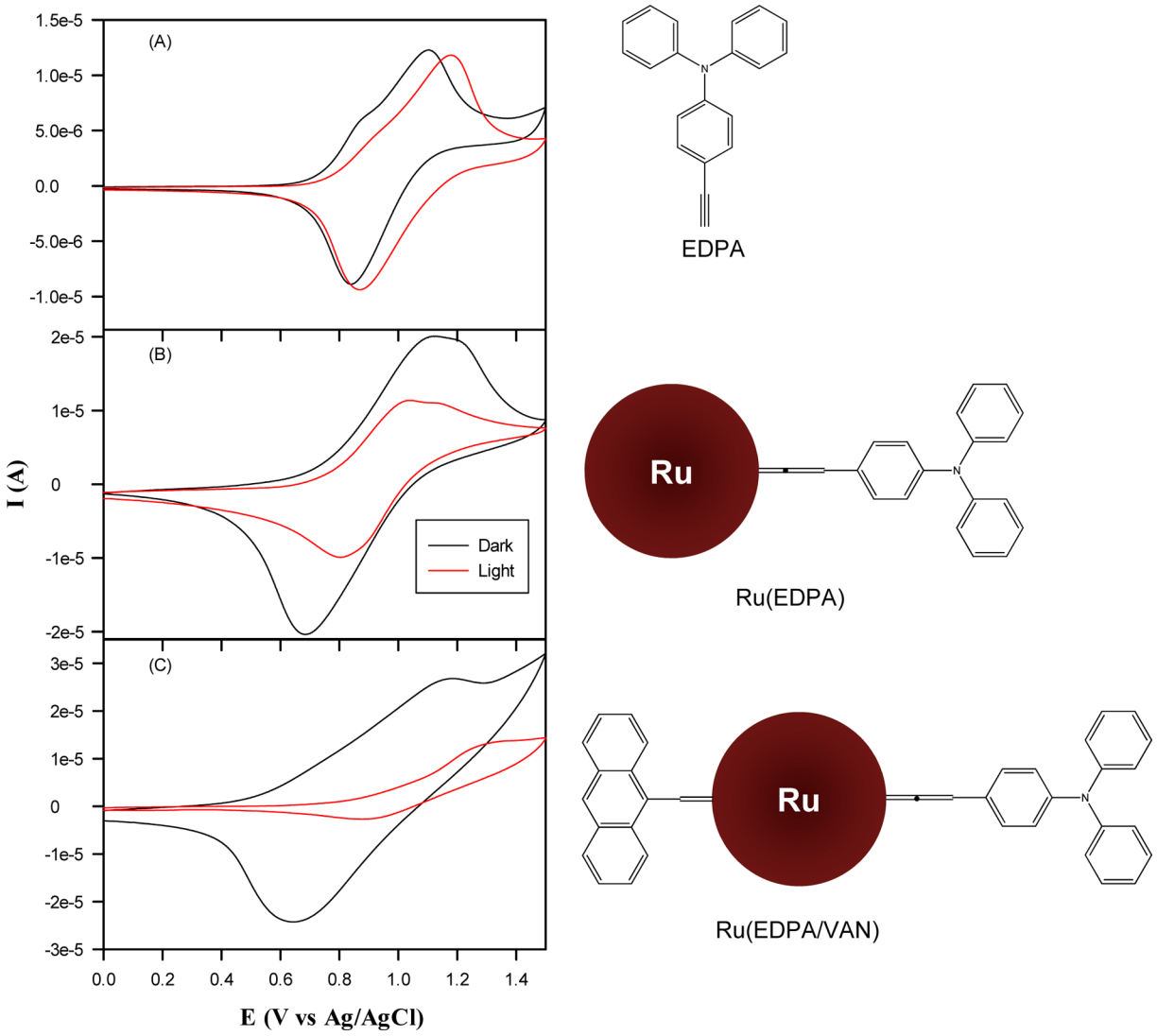

Figure 6. Cyclic voltammograms acquired in the dark (black curves) and under UV-photoirradiation (red curves) of (A) monomeric EDPA, (B) Ru(EDPA), and (C) Ru(EDPA/VAN) nanoparticles in CH_2Cl_2 with 0.1 M TBAP. The structures of the corresponding samples are shown on the right. Adapted with permission from ref 34. Copyright 2013 Royal Society of Chemistry.

(35.8% VAN and 25.2% EDPA) upon UV photoirradiation, as revealed in photoluminescence measurements where the emergence of new emissions suggests efficient mixing of the electronic energy levels of particle-bound triphenylamine and anthracene moieties. Such photoinduced intraparticle charge transfer in Ru(EDPA/VAN) nanoparticles is further confirmed in electrochemical measurements. As shown in Figure 6, although the Ru(EDPA/VAN) nanoparticles display a single pair of voltammetric peaks at $E^{\circ\prime}$ = +0.91 V in the dark, close to that of Ru(EDPA) (41% EDPA) nanoparticles, the peaks almost completely disappear under UV photoirradiation, whereas for Ru(EDPA) the peak currents diminish by about half. Note that the voltammetric currents are virtually unchanged with the EDPA monomers before and after UV photoirradiation. This may be ascribed to the transfer of photoexcited electrons from triphenylamine to metal cores and further to electron-accepting anthracene. That is, UV photoirradiation induces depletion of triphenylamine valence electrons, and consequently diminishes the corresponding voltammetric currents, in agreement with the photoluminescence results. Such a behavior is analogous to molecular dyads with conjugated chemical spacers, but different from those built on noncovalent interactions between organic molecules and metal nanoparticles.[71−74]

The conjugated metal−ligand interfacial bonds may also be exploited to manipulate the electron density of metal nanoparticles, a critical factor in nanoparticle electrocatalysis. This has been demonstrated in several recent studies where metal nanoparticles functionalized with acetylene derivatives exhibit enhanced electrocatalytic activity toward oxygen reduction reaction (ORR), a critical process at fuel cell cathode. These include AgAu,[23] AuPd,[24] and Cu nanoparticles.[22] The enhanced ORR activity is partly ascribed to extended spilling of nanoparticle core electrons into the organic capping layers as a result of the conjugated metal−ligand bonds. The subtle diminishment of the core electronic density leads to optimal binding to oxygen intermediates and hence enhanced ORR electrocatalytic activity, as manifested by the so-called volcano plot.[75−82] This is in line with the rich manipulation of ORR activity of nanoparticle catalysts by metal−ligand (substrate) interactions, as demonstrated in numerous studies in the literature.[38,83−89]

DOI: 10.1021/acs.accounts.6b00377
Acc. Chem. Res. 2016, 49, 2251−2260

CONCLUSIONS AND OUTLOOK

A variety of conjugated metal−ligand interfacial bonds have been formed for nanoparticle surface functionalization, where intraparticle charge delocalization occurs between nanoparticle-bound functional moieties, in contrast to the mercapto-capped counterparts. This leads to the emergence of new optical and electronic properties of the nanoparticles. Such an unprecedented level of control of the nanoparticles electronic properties may be exploited for diverse applications such as chemical sensing, (nano)electronics and electrocatalysis. In fact, there is a rich variety of metal-nonmetal bonds in organometallic chemistry. It is envisaged that such chemistry may be adopted for nanoparticle surface functionalization. For instance, in a prior study[90] we have demonstrated that metal nanoparticles may be functionalized with nitrene fragments using azide derivatives as the precursors, where new optical and electronic properties emerge with the formation of metal-nitrene (M═N) π bonds. Relevant research is ongoing.

AUTHOR INFORMATION

Notes

The authors declare no competing financial interest.

Biographies

Peiguang Hu received his B.E. degree in 2008 and M.S. degree in 2011 in Materials Science from Shandong University (China). In June 2016, he obtained his Ph.D. degree in Chemistry from the University of California, Santa Cruz (UCSC) under the supervision of Professor Shaowei Chen. His research is focused on metal nanoparticle surface functionalization and their applications in fuel cell electrocatalysis.

Limei Chen obtained her B.E. degree in 2009 and M.S. degree in 2012 in Materials Science from Shandong University. She is pursuing her Ph.D. degree at UCSC in Professor Shaowei Chen's laboratory. Her dissertation research is focused on functional nanoparticles by interfacial engineering and their electron-transfer chemistry.

Xiongwu Kang received his B.S. degree in Materials Science and Engineering from the University of Science and Technology of China (USTC) in 2007, and Ph.D. degree from UCSC in 2012 under the supervision of Professor Shaowei Chen. After a postdoctoral appointment at Georgia Institute of Technology with Professor M. A. El-Sayed, he started his independent research in South China University of Technology in 2015. His research interest includes surface functionalization of metal nanoparticles and applications in electrocatalysis and solar cells.

Shaowei Chen received his B.S. degree in Chemical Physics from USTC in 1991, and his M.S. and Ph.D. degrees from Cornell University in 1993 and 1996, respectively. Following a postdoctoral appointment in the University of North Carolina at Chapel Hill, he started his independent career in Southern Illinois University in 1998. In summer 2004, he moved to UCSC and is currently a Professor of Chemistry. He is interested in nanoscale functional materials and their electron transfer chemistry.

ACKNOWLEDGMENTS

This work was supported, in part, by grants from the National Science Foundation.

REFERENCES

(1) Zhou, Z. Y.; Kang, X. W.; Song, Y.; Chen, S. W. Butylphenyl-functionalized palladium nanoparticles as effective catalysts for the electrooxidation of formic acid. *Chem. Commun.* **2011**, *47*, 6075−6077.
(2) Ghosh, D.; Chen, S. W. Palladium nanoparticles passivated by metal-carbon covalent linkages. *J. Mater. Chem.* **2008**, *18*, 755−762.
(3) Chen, W.; Davies, J. R.; Ghosh, D.; Tong, M. C.; Konopelski, J. P.; Chen, S. W. Carbene-functionalized ruthenium nanoparticles. *Chem. Mater.* **2006**, *18*, 5253−5259.
(4) Chen, W.; Zuckerman, N. B.; Kang, X. W.; Ghosh, D.; Konopelski, J. P.; Chen, S. W. Alkyne-Protected Ruthenium Nanoparticles. *J. Phys. Chem. C* **2010**, *114*, 18146−18152.
(5) Kang, X.; Zuckerman, N. B.; Konopelski, J. P.; Chen, S. Alkyne-functionalized ruthenium nanoparticles: ruthenium-vinylidene bonds at the metal-ligand interface. *J. Am. Chem. Soc.* **2012**, *134*, 1412−1415.
(6) Mirkhalaf, F.; Paprotny, J.; Schiffrin, D. J. Synthesis of metal nanoparticles stabilized by metal-carbon bonds. *J. Am. Chem. Soc.* **2006**, *128*, 7400−7401.
(7) Kawai, K.; Narushima, T.; Kaneko, K.; Kawakami, H.; Matsumoto, M.; Hyono, A.; Nishihara, H.; Yonezawa, T. Synthesis and antibacterial properties of water-dispersible silver nanoparticles stabilized by metal-carbon sigma-bonds. *Appl. Surf. Sci.* **2012**, *262*, 76−80.
(8) Maity, P.; Takano, S.; Yamazoe, S.; Wakabayashi, T.; Tsukuda, T. Binding Motif of Terminal Alkynes on Gold Clusters. *J. Am. Chem. Soc.* **2013**, *135*, 9450−9457.
(9) Zhang, S.; Chandra, K. L.; Gorman, C. B. Self-assembled monolayers of terminal alkynes on gold. *J. Am. Chem. Soc.* **2007**, *129*, 4876−4877.
(10) Murray, R. W. Nanoelectrochemistry: Metal nanoparticles, nanoelectrodes, and nanopores. *Chem. Rev.* **2008**, *108*, 2688−2720.
(11) Shahid, G.; Sheppard, N. IR Spectra and the Structures of the Chemisorbed Species Resulting from the Adsorption of the Linear Butenes on a Pt/Sio_2 Catalyst. Part 1. Temperature Dependence of the Spectra. *J. Chem. Soc., Faraday Trans.* **1994**, *90*, 507−511.
(12) Sheppard, N. Vibrational Spectroscopic Studies of the Structure of Species Derived from the Chemisorption of Hydrocarbons on Metal Single-Crystal Surfaces. *Annu. Rev. Phys. Chem.* **1988**, *39*, 589−644.
(13) Crabtree, R. H. *Organometallic Chemistry of the Transition Metals*, 6th ed.; Wiley: Hoboken, NJ, 2014.
(14) Siegbahn, P. E. M. Trends of Metal-Carbon Bond Strengths in Transition-Metal Complexes. *J. Phys. Chem.* **1995**, *99*, 12723−12729.
(15) Simoes, J. A. M.; Beauchamp, J. L. Transition-Metal Hydrogen and Metal-Carbon Bond Strengths - the Keys to Catalysis. *Chem. Rev.* **1990**, *90*, 629−688.
(16) Ghosh, D.; Chen, S. W. Solid-state electronic conductivity of ruthenium nanoparticles passivated by metal-carbon covalent bonds. *Chem. Phys. Lett.* **2008**, *465*, 115−119.
(17) Chen, W.; Pradhan, S.; Chen, S. W. Photoluminescence and conductivity studies of anthracene-functionalized ruthenium nanoparticles. *Nanoscale* **2011**, *3*, 2294−2300.
(18) Kang, X. W.; Chen, S. W. Electronic conductivity of alkyne-capped ruthenium nanoparticles. *Nanoscale* **2012**, *4*, 4183−4189.
(19) Chen, W.; Chen, S. W.; Ding, F. Z.; Wang, H. B.; Brown, L. E.; Konopelski, J. P. Nanoparticle-mediated intervalence transfer. *J. Am. Chem. Soc.* **2008**, *130*, 12156−12162.
(20) Chen, W.; Brown, L. E.; Konopelski, J. P.; Chen, S. W. Intervalence transfer of ferrocene moieties adsorbed on electrode surfaces by a conjugated linkage. *Chem. Phys. Lett.* **2009**, *471*, 283−285.
(21) He, G. Q.; Song, Y.; Kang, X. W.; Chen, S. W. Alkyne-functionalized palladium nanoparticles: Synthesis, characterization, and electrocatalytic activity in ethylene glycol oxidation. *Electrochim. Acta* **2013**, *94*, 98−103.
(22) Liu, K.; Song, Y.; Chen, S. W. Electrocatalytic activities of alkyne-functionalized copper nanoparticles in oxygen reduction in alkaline media. *J. Power Sources* **2014**, *268*, 469−475.
(23) Hu, P. G.; Song, Y.; Chen, L. M.; Chen, S. W. Electrocatalytic activity of alkyne-functionalized AgAu alloy nanoparticles for oxygen reduction in alkaline media. *Nanoscale* **2015**, *7*, 9627−9636.
(24) Deming, C. P.; Zhao, A.; Song, Y.; Liu, K.; Khan, M. M.; Yates, V. M.; Chen, S. W. Alkyne-Protected AuPd Alloy Nanoparticles for

DOI: 10.1021/acs.accounts.6b00377
Acc. Chem. Res. 2016, 49, 2251−2260

Electrocatalytic Reduction of Oxygen. *ChemElectroChem* **2015**, *2*, 1719−1727.
(25) Hu, P. G.; Duchesne, P. N.; Song, Y.; Zhang, P.; Chen, S. W. Self-Assembly and Chemical Reactivity of Alkenes on Platinum Nanoparticles. *Langmuir* **2015**, *31*, 522−528.
(26) Hu, P. G.; Chen, L. M.; Deming, C. P.; Lu, J. E.; Bonny, L. W.; Chen, S. W. Effects of para-substituents of styrene derivatives on their chemical reactivity on platinum nanoparticle surfaces. *Nanoscale* **2016**, *8*, 12013−12021.
(27) Chen, W.; Zuckerman, N. B.; Lewis, J. W.; Konopelski, J. P.; Chen, S. W. Pyrene-Functionalized Ruthenium Nanoparticles: Novel Fluorescence Characteristics from Intraparticle Extended Conjugation. *J. Phys. Chem. C* **2009**, *113*, 16988−16995.
(28) Chen, L. M.; Hu, P. G.; Deming, C. P.; Li, W.; Li, L. G.; Chen, S. W. Chemical Reactivity of Naphthalenecarboxylate-Protected Ruthenium Nanoparticles: Intraparticle Charge Delocalization Derived from Interfacial Decarboxylation. *J. Phys. Chem. C* **2015**, *119*, 15449−15454.
(29) Chen, L. M.; Song, Y.; Hu, P. G.; Deming, C. P.; Guo, Y.; Chen, S. W. Interfacial reactivity of ruthenium nanoparticles protected by ferrocenecarboxylates. *Phys. Chem. Chem. Phys.* **2014**, *16*, 18736−18742.
(30) Kang, X. W.; Zuckerman, N. B.; Konopelski, J. P.; Chen, S. W. Alkyne-Stabilized Ruthenium Nanoparticles: Manipulation of Intraparticle Charge Delocalization by Nanoparticle Charge States. *Angew. Chem., Int. Ed.* **2010**, *49*, 9496−9499.
(31) Hu, P. G.; Chen, L. M.; Deming, C. P.; Kang, X. W.; Chen, S. W. Nanoparticle-Mediated Intervalence Charge Transfer: Core-Size Effects. *Angew. Chem., Int. Ed.* **2016**, *55*, 1455−1459.
(32) Kang, X. W.; Chen, W.; Zuckerman, N. B.; Konopelski, J. P.; Chen, S. W. Intraparticle Charge Delocalization of Carbene-Functionalized Ruthenium Nanoparticles Manipulated by Selective Ion Binding. *Langmuir* **2011**, *27*, 12636−12641.
(33) Kang, X. W.; Li, X.; Hewitt, W. M.; Zuckerman, N. B.; Konopelski, J. P.; Chen, S. W. Manipulation of Intraparticle Charge Delocalization by Selective Complexation of Transition-Metal Ions with Histidine Moieties. *Anal. Chem.* **2012**, *84*, 2025−2030.
(34) Phebus, B. D.; Yuan, Y.; Song, Y.; Hu, P. G.; Abdollahian, Y.; Tong, Q. X.; Chen, S. W. Intraparticle donor-acceptor dyads prepared using conjugated metal-ligand linkages. *Phys. Chem. Chem. Phys.* **2013**, *15*, 17647−17653.
(35) Chen, W.; Zuckerman, N. B.; Konopelski, J. P.; Chen, S. W. Pyrene-Functionalized Ruthenium Nanoparticles as Effective Chemosensors for Nitroaromatic Derivatives. *Anal. Chem.* **2010**, *82*, 461−465.
(36) Hu, P. G.; Song, Y.; Rojas-Andrade, M. D.; Chen, S. W. Platinum Nanoparticles Functionalized with Ethynylphenylboronic Acid Derivatives: Selective Manipulation of Nanoparticle Photoluminescence by Fluoride Ions. *Langmuir* **2014**, *30*, 5224−5229.
(37) Zhou, Z. Y.; Kang, X. W.; Song, Y.; Chen, S. W. Enhancement of the electrocatalytic activity of Pt nanoparticles in oxygen reduction by chlorophenyl functionalization. *Chem. Commun.* **2012**, *48*, 3391−3393.
(38) Zhou, Z. Y.; Kang, X. W.; Song, Y.; Chen, S. W. Ligand-Mediated Electrocatalytic Activity of Pt Nanoparticles for Oxygen Reduction Reactions. *J. Phys. Chem. C* **2012**, *116*, 10592−10598.
(39) Zhou, Z. Y.; Ren, J.; Kang, X.; Song, Y.; Sun, S. G.; Chen, S. Butylphenyl-functionalized Pt nanoparticles as CO-resistant electrocatalysts for formic acid oxidation. *Phys. Chem. Chem. Phys.* **2012**, *14*, 1412−1417.
(40) Chen, S. W.; Zhao, Z. H.; Liu, H. Charge Transport at the Metal-Organic Interface. *Annu. Rev. Phys. Chem.* **2013**, *64*, 221−245.
(41) Tulevski, G. S.; Myers, M. B.; Hybertsen, M. S.; Steigerwald, M. L.; Nuckolls, C. Formation of catalytic metal-molecule contacts. *Science* **2005**, *309*, 591−594.
(42) Baquero, E. A.; Tricard, S.; Flores, J. C.; de Jesus, E.; Chaudret, B. Highly Stable Water-Soluble Platinum Nanoparticles Stabilized by Hydrophilic N-Heterocyclic Carbenes. *Angew. Chem., Int. Ed.* **2014**, *53*, 13220−13224.
(43) Crudden, C. M.; Horton, J. H.; Ebralidze, I. I.; Zenkina, O. V.; McLean, A. B.; Drevniok, B.; She, Z.; Kraatz, H. B.; Mosey, N. J.; Seki, T.; Keske, E. C.; Leake, J. D.; Rousina-Webb, A.; Wu, G. Ultra stable self-assembled monolayers of N-heterocyclic carbenes on gold. *Nat. Chem.* **2014**, *6*, 409−414.
(44) MacLeod, M. J.; Johnson, J. A. PEGylated N-Heterocyclic Carbene Anchors Designed To Stabilize Gold Nanoparticles in Biologically Relevant Media. *J. Am. Chem. Soc.* **2015**, *137*, 7974−7977.
(45) Vignolle, J.; Tilley, T. D. N-Heterocyclic carbene-stabilized gold nanoparticles and their assembly into 3D superlattices. *Chem. Commun.* **2009**, 7230−7232.
(46) Creutz, C.; Taube, H. Binuclear complexes of ruthenium ammines. *J. Am. Chem. Soc.* **1973**, *95*, 1086−1094.
(47) Powers, M. J.; Meyer, T. J. Intervalence transfer in mixed-valence biferrocene ions. *J. Am. Chem. Soc.* **1978**, *100*, 4393−4398.
(48) Robin, M. B.; Day, P. Mixed valence chemistry. A survey and classification. *Adv. Inorg. Chem. Radiochem.* **1968**, *10*, 247−422.
(49) Nelsen, S. F. ″Almost delocalized″ intervalence compounds. *Chem. - Eur. J.* **2000**, *6*, 581−588.
(50) Demadis, K. D.; Hartshorn, C. M.; Meyer, T. J. The localized-to-delocalized transition in mixed-valence chemistry. *Chem. Rev.* **2001**, *101*, 2655−2685.
(51) Cowan, D. O.; Levanda, C.; Park, J.; Kaufman, F. Organic Solid-State 0.8. Mixed-Valence Ferrocene Chemistry. *Acc. Chem. Res.* **1973**, *6*, 1−7.
(52) Warta, R.; Sixl, H. Optical-Absorption and Fluorescence Spectroscopy of Stable Diacetylene Oligomer Molecules. *J. Chem. Phys.* **1988**, *88*, 95−99.
(53) Patterson, M. L.; Weaver, M. J. Surface-Enhanced Raman-Spectroscopy as a Probe of Adsorbate Surface Bonding - Simple Alkenes and Alkynes Adsorbed at Gold Electrodes. *J. Phys. Chem.* **1985**, *89*, 5046−5051.
(54) Ford, M. J.; Hoft, R. C.; McDonagh, A. Theoretical study of ethynylbenzene adsorption on Au(111) and implications for a new class of self-assembled monolayer. *J. Phys. Chem. B* **2005**, *109*, 20387−20392.
(55) Li, Q.; Han, C. B.; Fuentes-Cabrera, M.; Terrones, H.; Sumpter, B. G.; Lu, W. C.; Bernholc, J.; Yi, J. Y.; Gai, Z.; Baddorf, A. P.; Maksymovych, P.; Pan, M. H. Electronic Control over Attachment and Self-Assembly of Alkyne Groups on Gold. *ACS Nano* **2012**, *6*, 9267−9275.
(56) Feilchenfeld, H.; Weaver, M. J. Binding of Alkynes to Silver, Gold, and Underpotential-Deposited Silver Electrodes as Deduced by Surface-Enhanced Raman-Spectroscopy. *J. Phys. Chem.* **1989**, *93*, 4276−4282.
(57) Nykanen, L.; Hakkinen, H.; Honkala, K. Computational study of linear carbon chains on gold and silver surfaces. *Carbon* **2012**, *50*, 2752−2763.
(58) Boronat, M.; Combita, D.; Concepcion, P.; Corma, A.; Garcia, H.; Juarez, R.; Laursen, S.; de Dios Lopez-Castro, J. Making C-C Bonds with Gold: Identification of Selective Gold Sites for Homo- and Cross-Coupling Reactions between Iodobenzene and Alkynes. *J. Phys. Chem. C* **2012**, *116*, 24855−24867.
(59) Joo, S.-W.; Kim, K. Adsorption of phenylacetylene on gold nanoparticle surfaces investigated by surface-enhanced Raman scattering. *J. Raman Spectrosc.* **2004**, *35*, 549−554.
(60) Chen, S. W.; Ingram, R. S.; Hostetler, M. J.; Pietron, J. J.; Murray, R. W.; Schaaff, T. G.; Khoury, J. T.; Alvarez, M. M.; Whetten, R. L. Gold nanoelectrodes of varied size: Transition to molecule-like charging. *Science* **1998**, *280*, 2098−2101.
(61) Peng, Y.; Deming, C. P.; Chen, S. Intervalence Charge Transfer Mediated by Silicon Nanoparticles. *ChemElectroChem* **2016**, *3*, 1219−1224.
(62) Peng, Y.; Lu, J. E.; Deming, C. P.; Chen, L.; Wang, N.; Hirata, E. Y.; Chen, S. Photo-Gated Intervalence Charge Transfer of Ethynylferrocene Functionalized Titanium Dioxide Nanoparticles. *Electrochim. Acta* **2016**, *211*, 704−710.
(63) Bothra, S.; Solanki, J. N.; Sahoo, S. K. Functionalized silver nanoparticles as chemosensor for pH, He^{2+} and Fe^{3+} in aqueous medium. *Sens. Actuators, B* **2013**, *188*, 937−943.

DOI: 10.1021/acs.accounts.6b00377
Acc. Chem. Res. 2016, 49, 2251−2260

(64) Salvia, M. V.; Ramadori, F.; Springhetti, S.; Diez-Castellnou, M.; Perrone, B.; Rastrelli, F.; Mancin, F. Nanoparticie-Assisted NMR Detection of Organic Anions: From Chemosensing to Chromatography. *J. Am. Chem. Soc.* **2015**, *137*, 886−892.
(65) Perrone, B.; Springhetti, S.; Ramadori, F.; Rastrelli, F.; Mancin, F. "NMR Chemosensing" Using Monolayer-Protected Nanoparticles as Receptors. *J. Am. Chem. Soc.* **2013**, *135*, 11768−11771.
(66) McFarland, A. D.; Van Duyne, R. P. Single silver nanoparticles as real-time optical sensors with zeptomole sensitivity. *Nano Lett.* **2003**, *3*, 1057−1062.
(67) Cheng, Z. H.; Li, G.; Zhang, N.; Liu, H. O. A novel functionalized silver nanoparticles solid chemosensor for detection of Hg(II) in aqueous media. *Dalton Trans* **2014**, *43*, 4762−4769.
(68) Lee, H. Y.; Son, H.; Lim, J. M.; Oh, J.; Kang, D.; Han, W. S.; Jung, J. H. BODIPY-functionalized gold nanoparticles as a selective fluoro-chromogenic chemosensor for imaging Cu^{2+} in living cells. *Analyst* **2010**, *135*, 2022−2027.
(69) Raymo, F. M.; Tomasulo, M. Electron and energy transfer modulation with photochromic switches. *Chem. Soc. Rev.* **2005**, *34*, 327−336.
(70) Lin, Y. Z.; Li, Y. F.; Zhan, X. W. Small molecule semiconductors for high-efficiency organic photovoltaics. *Chem. Soc. Rev.* **2012**, *41*, 4245−4272.
(71) Angioni, A.; Corni, S.; Mennucci, B. Can we control the electronic energy transfer in molecular dyads through metal nanoparticles? A QM/continuum investigation. *Phys. Chem. Chem. Phys.* **2013**, *15*, 3294−3303.
(72) Kotiaho, A.; Lahtinen, R.; Lemmetyinen, H. Photoinduced processes in chromophore-gold nanoparticle assemblies. *Pure Appl. Chem.* **2011**, *83*, 813−821.
(73) Kotiaho, A.; Lahtinen, R. M.; Tkachenko, N. V.; Efimov, A.; Kira, A.; Imahori, H.; Lemmetyinen, H. Gold nanoparticle enhanced charge transfer in thin film assemblies of porphyrin-fullerene dyads. *Langmuir* **2007**, *23*, 13117−13125.
(74) Xu, J. P.; Jia, L.; Fang, Y. A.; Lv, L. P.; Song, Z. G.; Ji, J. A. Highly soluble PEGylated pyrene-gold nanoparticles dyads for sensitive turn-on fluorescent detection of biothiols. *Analyst* **2010**, *135*, 2323−2327.
(75) Stephens, I. E. L.; Bondarenko, A. S.; Grønbjerg, U.; Rossmeisl, J.; Chorkendorff, I. Understanding the electrocatalysis of oxygen reduction on platinum and its alloys. *Energy Environ. Sci.* **2012**, *5*, 6744−6762.
(76) Kitchin, J. R.; Norskov, J. K.; Barteau, M. A.; Chen, J. G. Modification of the surface electronic and chemical properties of Pt(111) by subsurface 3d transition metals. *J. Chem. Phys.* **2004**, *120*, 10240−10246.
(77) Lima, F. H. B.; Zhang, J.; Shao, M. H.; Sasaki, K.; Vukmirovic, M. B.; Ticianelli, E. A.; Adzic, R. R. Catalytic Activity-d-Band Center Correlation for the O2 Reduction Reaction on Platinum in Alkaline Solutions. *J. Phys. Chem. C* **2007**, *111*, 404−410.
(78) Hammer, B.; Norskov, J. K. Electronic factors determining the reactivity of metal surfaces. *Surf. Sci.* **1995**, *343*, 211−220.
(79) Hennig, D.; GandugliaPirovano, M. V.; Scheffler, M. Adlayer core-level shifts of admetal monolayers on transition-metal substrates and their relation to the surface chemical reactivity. *Phys. Rev. B: Condens. Matter Mater. Phys.* **1996**, *53*, 10344−10347.
(80) Bzowski, A.; Sham, T. K.; Watson, R. E.; Weinert, M. Electronic-Structure of Au and Ag Overlayers on Ru(001) - the Behavior of the Noble-Metal D-Bands. *Phys. Rev. B: Condens. Matter Mater. Phys.* **1995**, *51*, 9979−9984.
(81) Weinert, M.; Watson, R. E. Core-Level Shifts in Bulk Alloys and Surface Adlayers. *Phys. Rev. B: Condens. Matter Mater. Phys.* **1995**, *51*, 17168−17180.
(82) Toyoda, E.; Jinnouchi, R.; Hatanaka, T.; Morimoto, Y.; Mitsuhara, K.; Visikovskiy, A.; Kido, Y. The d-Band Structure of Pt Nanoclusters Correlated with the Catalytic Activity for an Oxygen Reduction Reaction. *J. Phys. Chem. C* **2011**, *115*, 21236−21240.
(83) Tsunoyama, H.; Ichikuni, N.; Sakurai, H.; Tsukuda, T. Effect of Electronic Structures of Au Clusters Stabilized by Poly(N-vinyl-2-pyrrolidone) on Aerobic Oxidation Catalysis. *J. Am. Chem. Soc.* **2009**, *131*, 7086−7093.
(84) Udumula, V.; Tyler, J. H.; Davis, D. A.; Wang, H.; Linford, M. R.; Minson, P. S.; Michaelis, D. J. Dual Optimization Approach to Bimetallic Nanoparticle Catalysis: Impact of M-1/M-2 Ratio and Supporting Polymer Structure on Reactivity. *ACS Catal.* **2015**, *5*, 3457−3462.
(85) Zhou, Z.-Y.; Chen, S. W. Impacts of Surface Functionalization on the Electrocatalytic Activity of Noble Metals and Nanoparticles. In *Molecular Interactions*; Meghea, A., Ed.; InTech: Vienna, Austria, 2012; pp 105−124.
(86) He, G.; Song, Y.; Liu, K.; Walter, A.; Chen, S.; Chen, S. Oxygen Reduction Catalyzed by Platinum Nanoparticles Supported on Graphene Quantum Dots. *ACS Catal.* **2013**, *3*, 831−838.
(87) Song, Y.; Chen, S. Graphene quantum-dot-supported platinum nanoparticles: defect-mediated electrocatalytic activity in oxygen reduction. *ACS Appl. Mater. Interfaces* **2014**, *6*, 14050−14060.
(88) Liu, K.; Song, Y.; Chen, S. W. Oxygen reduction catalyzed by nanocomposites based on graphene quantum dots-supported copper nanoparticles. *Int. J. Hydrogen Energy* **2016**, *41*, 1559−1567.
(89) Deming, C. P.; Mercado, R.; Gadiraju, V.; Sweeney, S. W.; Khan, M.; Chen, S. Graphene Quantum Dots-Supported Palladium Nanoparticles for Efficient Electrocatalytic Reduction of Oxygen in Alkaline Media. *ACS Sustainable Chem. Eng.* **2015**, *3*, 3315−3323.
(90) Kang, X. W.; Song, Y.; Chen, S. W. Nitrene-functionalized ruthenium nanoparticles. *J. Mater. Chem.* **2012**, *22*, 19250−19257.

DOI: 10.1021/acs.accounts.6b00377
Acc. Chem. Res. 2016, 49, 2251−2260